DOI: 10.13009/EUCASS2019-192

Using Pulsed Laser Ranging to Drastically Improve LEO Orbit Ephemerii

Claude Phipps and Christophe Bonnal***
**Photonic Associates, LLC*
200A Ojo de la Vaca Road, Santa Fe, NM 87508 USA, crphipps@aol.com
***CNES, Direction des Lanceurs*
52 rue Jacques Hilairet, 75612 Paris Cedex, France, Christophe.bonnal@cnes.fr

Abstract
We propose an orbiting pulsed laser station with a high sensitivity, high data rate detector array to improve orbital location precision to 10cm relative to Earth coordinates. The station will use a 5m focal length, 50cm diameter optic feeding an 85% efficient, 1Gpixel gated array to establish tracks in sunlight. In staring mode, it tracks objects with solar illumination down to 1cm in size at 250km range. The system then actively tracks selected objects using a 50mJ, 100ps, 50Hz repetitive-pulse laser. N data points per satellite encounter with m encounters over several days improves accuracy of the determined orbit.

1. Introduction

A long-living legacy of space junk larger than 50-100cm, and with 500-1000kg mass reminds us of the danger of collisions and the importance of predicting those accurately in advance. For these objects, present accuracy of orbit ephemerii is inadequate. A position uncertainty of order 1km leads to an unacceptable 99.9% false alarm rate for predicted mutual collisions [1]. In contrast, 100ps pulses permit ranging on any component of a spacecraft with 3cm precision.

As of this writing, 68 new satellite constellations have been approved for Low-Earth-Orbit (LEO), comprising 13,529 individual satellites. Noteworthy among these is the Starlink broadband constellation proposed by SpaceX, involving thousands of satellites whose deployment has been approved by the U.S. Federal Communications Commission [2]. These would be in 83 orbital planes in five separate altitude shells from 340 to 1100km. These will be 100-500-kg objects, the size of an office desk. SpaceX expects this network to reach 12,000 satellites by mid 2024 – by itself, a number more than six times the number of operational satellites now in orbit. Smith [3] points out that each week, 3,000 space objects have a conjunction closer than 1km in LEO.

The good news is that more than 90% of these satellites will propel themselves to a disposal orbit and re-enter at end of life, or decay naturally. However, during their lives, their presence at altitudes up to 1300 km would increase the density of objects in that altitude band by a factor of 7. Inevitably, some of these will become derelicts, joining the 4,000 other pieces of meter-size space junk in LEO. We must be able to precisely determine the orbits of these objects as they become uncontrolled.

To accomplish this, we propose an orbiting pulsed laser station with a high sensitivity, high data rate detector array to improve orbital center-of-mass range precision to 10cm relative to the station (Fig. 1). Its detector array can also determine transverse location with 45cm precision at 1000km range and proportionally less at shorter range.

Periodically, the station's absolute position is determined to by 3 Earth-based stations "pinging" a retroreflector on the station with 100ps pulses simultaneously. The station is also equipped with GPS to assist in the position determination procedure. In this way, the orbit of every satellite it is able to study is determined absolutely with respect to Earth coordinates with at least 10cm accuracy.

The station will use a 5m focal length, 50cm diameter optic feeding a 1.5Gpixel gateable array of 2.5μm pixels with 85% photoelectric efficiency in the visible to establish tracks in sunlight. Its field of view is narrow, 1 degree. In staring mode, it will permit tracking objects with solar illumination down to 15cm in size at 1000km range, and 1cm at 250km.

DOI: 10.13009/EUCASS2019-192

Having established a track, the electro-optical system then does active rather than passive tracking on a selected object using a 50mJ, 100ps, 1.06µm, 50Hz, 2.5W repetitive-pulse laser. N such data points per satellite encounter with m encounters over several days improves accuracy further and permits orbit determination. At 1000km range, only 32µJ/cm^2 is incident on targets, a fluence level that cannot cause damage to any materials unless further focused. This fluence can be maintained at shorter range by turning down the laser. Range gating together with a 50nm narrowband optical filter gives adequate signal/background ratios on most targets. Multiple stations are envisioned to increase coverage and data rate.

At the conclusion we briefly review large debris target management (LDTM) using lasers [4], a different system which would only be used on defunct satellites, to prevent collisions by gentle nudging over a period of 5-7 days in advance. At the outset, this would use a 532nm, 100J, 8Hz, 100ps laser adapted from the proposed "L'ADROIT" system [5], [6]. The two systems are synergistic, in that the LDTM laser can use lower power when ephemeris accuracy for these large objects is improved by a factor of 100 as a result of our spaceborne laser ranging proposal.

Please see Appendix I for a symbol glossary.

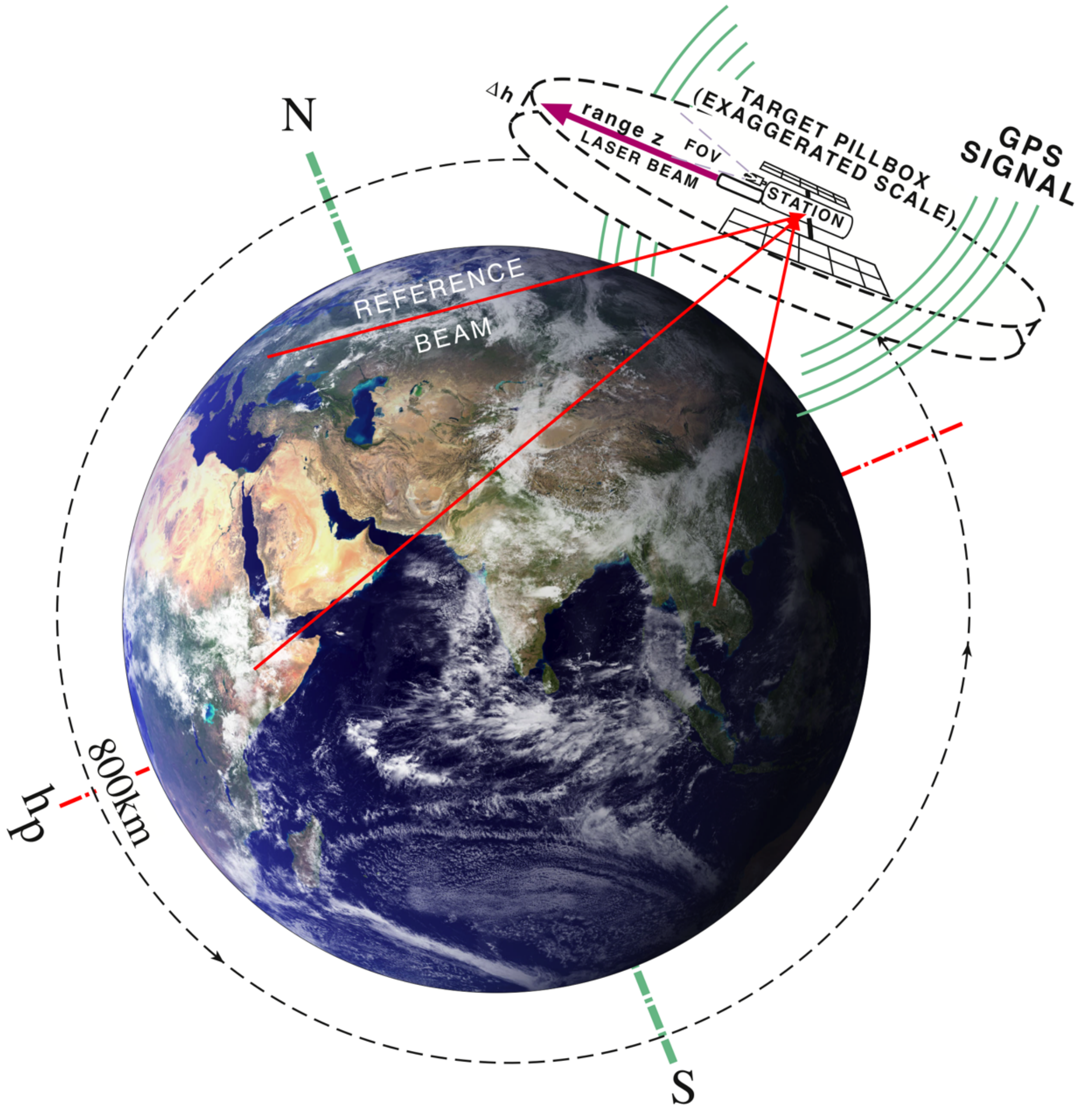

Figure 1. Laser Station

A first generation station would operate on debris whose orbits are most well known, such as large French debris. Second generation stations will then operate on other large debris. After these stations have reduced the position uncertainty of all dangerous large debris, the LDTM nudging station would be placed in orbit to prevent collisions with active spacecraft in real time.

DOI: 10.13009/EUCASS2019-192

2. Laser and Parameters for a Single System of the Ranging Array

One orbiting station can only provide precise location information on a given satellite in one dimension in one interaction, together with more coarse location information on the order of 1m in the transverse plane. At 50Hz, we obtain a large number N of data points in one encounter. In m encounters, enough data to determine an orbit for one object is gathered. The station consists of a laser system and a detection system. The laser system is small and inexpensive (Table 1), so it makes sense to have a swarm of stations in different planes and altitude bands working cooperatively to develop orbits for all objects of interest more rapidly than possible for a single station. Cost is about $136k [8].

Table 1: Ranging Laser Parameters

	Value	**Dimensions**
Wavelength	532	nm
Pulse energy	50	mJ
Pulse duration	100	ps
Repetition rate	50	Hz
Laser optical power	2.5	W
Laser beam quality M^2	2	----

The detection system uses a 5m focal length, 50cm diameter mirror together with a 1.54Gpixel array of 2.2μm detector elements (Table 2) to achieve a 1 degree field of view. The array is gated to sharply reduce background and increase signal to background ratio. Cost of the ranging laser (Example: EKSPLA PL2231A) is about $135k [8].

Table 2: Detection System Parameters

	Value	**Dimensions**
Center wavelength	550	nm
Optic diameter	50	cm
Focal length	5	m
Field of view	1	deg
Field of view	17	mrad
N pixels	1.54E9	----
Pixel size	2.23	μm
Array diameter (concave)	8.7	cm
Detector electric efficiency	85	%
Dark current at 20°C [7]	0.4	e/pixel/ms
Design use range	1000	km
Spot size at range	45	cm
Optical filter bandwidth	100	nm
Gate and refresh time	6.7	ms

In Table 3 we show the results of operation on a target with 25% diffuse reflectance into one sterradian, a typical value for aluminium. Note that spectral reflections are ignored in this analysis, and can only give better results than diffuse reflections. The station has two operating modes. In the first (Table 3), the station is normally staring, the laser is off and multiple tracks are created on the array with solar illumination of targets. Parameters employed in the table are based on [5]. In this mode, at 1000km, a target can cross the field of view in as little as 2.3s.

DOI: 10.13009/EUCASS2019-192

Table 3: Predicted Operating Parameters: Passive, Staring, Sun-illuminated

	Value	**Dimensions**
Range to target	1000	km
Target diffuse reflectivity R_λ	25	% per sterradian
Assumed range z	1000	km
Assumed target size	45	cm
Sun spectral brightness on target I_λ	1000	W/(m^{2}sterrad-μm)
Background spectral brightness*	1E-6	W/(m^{2}sterrad-μm)
Bandwidth	1	μm
Signal S	6.2	pW
Background B	25	zW
Signal/Background	2.5E8	----
Maximum target transverse velocity at range	7500	m/s
Minimum target transit time per pixel	59	μs
Photoelectron number N_{pe}	866	----
Corresponding signal stability 1/SQRT(N_{pe})	3.4	%
Minimum size target that can be seen at 1000km	15	cm
Minimum size target that can be seen at 250km	1	cm
*in LEO above 300km, sun behind us, not looking down at Earth		

Then, the laser is activated and a particular target tracked (Figure 2, Table 4). In both tables, “stability” refers to the stability (shot noise) of the return signal, which we take to be unacceptable at N_{pe}=100 (10%). We see that the signal is easily large enough to overwhelm electrical “shot” noise in the detector.

Table 4: Predicted Operating Parameters: Active, Tracking, Gated, Filtered, Laser-illuminated

	Value	**Dimensions**
Range to target	1000	km
Target diffuse reflectivity R_λ	25	% per sterradian
Assumed range z	1000	km
Assumed target size	45	cm
Optic diameter	50	cm
Optic focal length	5	m
Laser spectral brightness on target I_λ	320	GW/(m^{2}sterrad-μm)
Background spectral brightness*	1.0	μW/(m^{2}sterrad-μm)
Gate time =2z/c	6.7	ms
Bandwidth limited by filter	100	nm
Signal	20	μW
Background	25	zW
Signal/Background	8.0E14	----
Signal energy W_S	2.0E-15	J
Background energy W_B	1.7E-24	J
Signal to background energy ratio W_S/W_B	1.2E9	----
Photoelectron number N_{pe}	4,680	----
Target R_λ for N_{pe}=100 at range z	0.005	% per sterradian
Target size for N_{pe}=100 at range z	6.9	cm
Signal stability (shot noise) 1/SQRT(N_{pe})	1.5	%

DOI: 10.13009/EUCASS2019-192

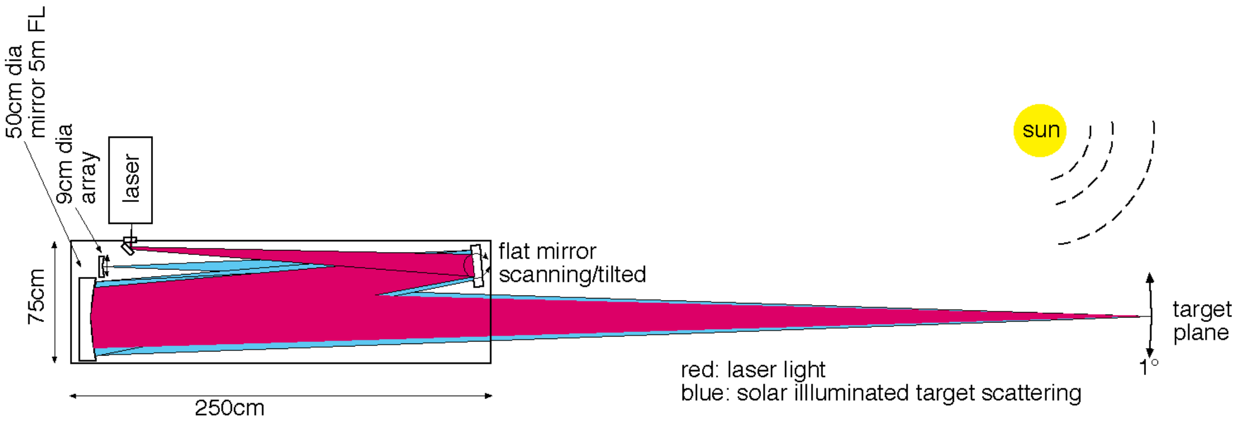

Figure 2. Laser and Telescope

Mirror tilts for ranging laser target illumination. Otherwise, it scans the target plane with a 1 degree field of view. The telescope shell is 75cm diameter and 2.5m long. Data analysis is located elsewhere in the station.

3. Large Debris Traffic Management and Nudging with Pulsed Lasers

At present there are 17,000 objects large enough to track (>10cm) in low-to-medium Earth orbit (LEO/MEO). Of these, 4,000 are uncontrolled multi-ton debris, including rocket bodies with residual fuel. Because they are not controlled these are a hazard to active satellites. But because they are tracked and their orbit ephemerii exist, impending collisions can be predicted days in advance. We showed in [4] that a single pulsed laser station in a slightly elliptical sunsynchronous orbit and oriented 6-18H to always face the sun, at a mean altitude of 900km with a 1.8kW average power capability can cause a 4-ton object to miss a collision by 1km, given 2 days advance warning. It's important to realize that the parameters for this system (Table 5) were based on the large position uncertainty inherent in present-day orbit parameters. We are not proposing to build an LDTM system in this paper, only a system to locate defunct orbital debris precisely.

We used the analogy of "sheep" to be herded, and estimated that there are about 1,230 "sheep" at this time, which need nudging at about one per day. We found the change in the period of a target with mass M from illuminating it in-plane with laser power P and coupling coefficient C_m is given by Eq. (1).

$$\Delta T = \mp 12\pi P C_m \tau \left(\frac{a^2}{M\mu} \right). \tag{1}$$

In Eq. (1), μ is the Earth's gravitation constant and a is the semimajor axis of the target orbit. The requirements for the laser station with 1km debris position uncertainty are shown in Table 5 [4].

When the Phase II ranging system we propose has reduced the position uncertainty to the order of 10cm, Table 6 shows how significantly the parameters of a LDTM nudging station can be relaxed, relative to Table 5. Because position uncertainties have been reduced by a factor of 100 relative to Table 5, we could propose a miss distance of 10m. However, we decided to be very conservative, with 100m miss distance. Also, we apply the laser pulses one week ahead of an impending conjunction, rather than just 2 days, and use a more realistic example of a 1-tonne debris target rather than 4 tonnes. Finally we use the second harmonic (530nm) rather than the third (355nm).

In Table 6, we take 10m miss distance as being a safe value given the new precision with which debris orbits are known. The correction we apply is followed in real-time, closed loop, to avoid unintended outcomes. Design parameters are based on [12], [13], [16] and [19]. Other applications are discussed in [15] and [18]. The most successful laser propelled flight to date is reported in [14].

DOI: 10.13009/EUCASS2019-192

Table 5: Requirements for LDTM laser nudging station based on 1km debris position uncertainty

	Value	**Dimensions**
Pulse energy W	3.0	kJ
Wavelength	355	nm
Rep rate f	0.6	Hz
Short term average optical power	1830	W
Burst duration (1 burst, 44 pulses per target)	73	s
Burst energy	133	kJ
Pulse duration	100	ps
Long term laser average power	4.2	W
Assumed target C_m	30E-6	N/W
Optic diameter	2	m
Laser range z	1500	km
Assumed target mass	4000	kg
Applied Δv during burst	1	mm/s
Resulting miss distance	37	m/orbit
Miss distance in 2 days	1	km

The single pulse energy listed in Tables 5 and 6 is required to achieve optimum coupling (lighting a plasma) on the distant target with the focusing optic diameter and laser range listed.

Table 6: Requirements for LDTM laser nudging station based on 10cm debris position uncertainty

	Value	**Dimensions**
Pulse energy W (2 pulses per burst)	480	J
Wavelength	532	nm
Pulse duration	100	ps
Long term laser average power in 2 days	1.5	mW
Assumed target C_m	30E-6	N/W
Optic diameter	2	m
Laser range z	400	km
Assumed target mass	1000	kg
Applied Δv during burst	29	μm/s
Resulting miss distance	1.1	m/orbit
Miss distance in 7 days	100	m

3.1. Optimum Fluence

It is important to note that "optimum" laser fluence on target depends on our goal. If it is maximum force per watt of laser light, as in this work, then about 35kJ/m^2 is best [11]. If, on the other hand, the goal is maximum ablation efficiency for minimum fuel mass use on long flights, earlier experimental work by Phipps [17] shows that a higher value of 350-600 kJ/m^2 can achieve near 100% ablation efficiency – at least for for metals – a value supported by new calculations by Tahan [18]. Experimental data on ablation efficiency are rare, and sorely needed.

5. Conclusions

The predicted evolution of the orbital population in the coming years exacerbates the need for efficient collision avoidance in orbit. Today, maneuvering active satellites to prevent a collision with a cataloged object is a routine

DOI: 10.13009/EUCASS2019-192

operation, but suffers from a huge rate of false alarms. As an example, the anti-collision service CAESAR from CNES monitors 105 satellites; it had to deal with more than 3 million Conjunction Messages in 2018, leading to 17 effective maneuvers. The situation will probably not improve with the deployment of large constellations, flocks of nanosatellites, and commissioning of the new large radar Space Fence which will potentially multiply by a factor 10.

A drastic improvement of the precision of ephemerii is compulsory to reduce the number of false alarms, both for conventional Collision Avoidance, in orbit or at launch, but also for Just in time Collision Avoidance (JCA) in near future, preventing collisions between two large derelicts [6, 9].

The proposal we make is a stepped approach.

The first step would be the development of a small orbital laser ranging system for demonstration purpose. It will only target large known French debris such as old Ariane 1-4 upper stages or observation satellites in order to cope with any potential legal restrictions, and the results of the experiments would be compared to the well known ephemerii established by the French SST system COSMOS based on the Graves radar [10].

Once this proof of feasibility is achieved, a first laser ranging station can be developed. It is compatible in size and mass with a dual launch with the European Vega launcher, thus minimizing the overall costs and would be launched in a Sun-Synchronous orbit. The laser station will start collecting information on catalogued debris, assuming a global legal agreement would be achieved in order to allow such kind of operations; the gains coming from such operations should be such that it surely will be considered as general interest, therefore allowable. Only cataloged objects recognized as derelict would be considered; as we would use an initial pointing coming from known ephemerii, the risk of wrongly pinging an active satellite is very remote. This station would gather a very large number of information, continuously, and the treatment of such big data on ground has to be studied. Depending on the effective performances, it could be useful to have more than one station.

The third step corresponds to the development of a slightly larger station enabling small orbital changes to potentially hazardous debris; this Large Debris Traffic Management (LDTM) system will be coupled with the laser ranging function in order to minimize the rate of false alarms. Thanks to the increased precision of ephemerii, the requirement in terms of pulse energy remains low.

The ultimate step would be the use of such systems to modify significantly the orbit of large derelicts, such as old GEO satellites, as previously proposed in the L'ADROIT descriptions.

References

[1] H. Krag, S. Setty, A. di Mira. I. Zayer and T. Flohrer, "Ground-based laser for tracking and remediation – an architectural view," paper IAC-18-A6.7.1, 69th International Astronautical Congress, Bremen 1-5 October 2018

[2] Irene Klotz, "Showdown at LEO," Aviation Week and Space Technology, pp. 50-53, May 6-19, 2019

[3] C. Smith, "Remote manoeuvre of space debris using photon pressure for active collision avoidance," Paper 7.2, Fifth European Workshop on Space Debris Modeling and Remediation (2018)

[4] C. Phipps, C. Bonnal and F. Masson, "Using lasers for large debris traffic management," paper 7.6, Proc. 5th Workshop on Space Debris Modeling and Remediation," CNES-HQ, Paris (2018)

[5] C. Phipps, "L'ADROIT - A spaceborne ultraviolet laser system for space debris clearing," *Acta Astro* **104**, 243-255 (2014)

[6] C. Phipps and C. Bonnal, "A spaceborne, pulsed UV laser system for re-entering or nudging LEO debris, and re-orbiting GEO debris," *Acta Astronautica* **118**, 224-236 (2016)

[7] based on published specifications of Fairchild Imaging CCD456

[8] Estimate by S. Guthrie, Altos Photonics, 25 June 2019 (private communication)

[9] A. Jarry, Ch. Bonnal et al., "SRM plume: A candidate as space debris braking system for Just-In-Time Collision avoidance maneuver," *Acta Astronautica* **158**, 185–197 (2019)

[10] IAA Situation Report on Space Debris, http://www.iaaweb.org/iaa/Scientific%20Activity/sg514finalreport.pdf

[11] C. Phipps, M. Boustie ,J.-M. Chevalier, S. Baton, E. Brambrink, L. Berthe, M. Schneider, L. Videau, S. A. E. Boyer and S. Scharring, "Laser Impulse Coupling measurements at 400fs and 80ps using the LULI facility at 1057nm wavelength," J. Appl. Phys., 122, 193103, doi:10.1063/1.4997196 (2017)

DOI: 10.13009/EUCASS2019-192

[12] S. Oriol, F. Masson, S. Mazouffre, S. A. E. Boyer, S. Batom, M. Boustie, A. Alemany, C. Phipps and B. Tuchming, “Plasma propulsion: overview for launcher applications in the advanced concepts of the CNES launchers directorate,” paper 1063, 8th European Conference for Aeronautics and Space Sciences, Madrid 1-4 July (2019)

[13] S. A. E. Boyer, M. Boustie, L. Berthe, S. Baton, E. Brambrink, L. Videau, C. Rousseau, J.-M. Chevalier, C. Phipps, F. Masson, S. Oriol and C. Bonnal, “New advances in short-pulse laser for LEO environment,” paper 1062, 8th European Conference for Aeronautics and Space Sciences, Madrid 1-4 July (2019)

[14] L. Myrabo, “World record flights of beam-riding rocket lightcraft – demonstration of “disruptive” propulsion technology, paper AIAA 01-3798, 37th Joint Propulsion Conference and Exhibit, *Proc. AIAA* (2001) https://doi.org/10.2514/6.2001-3798

[15] T. Ebisuzaki, S. Wada, P. Gorodetzky, M. Battisti, H. Miyamoto, R. Vigna Cit, M. Bertaina, G. Suino, F. Fenu, K. Shinozaki and F. Bisconti, “Deorbiting mission of cm-sized space debris by laser ablation,” Paper 7.4, Fifth European Workshop on Space Debris Modeling and Remediation (2018)

[16] S. Boyer, A. Burr, S. Jacomet, M. Boustie, L. Berthe, S. Baton, E. Brambrink, L. Videau, J.-M. Chevalier, M. Schneider, C. Phipps, F. Masson and C. Bonnal, “400fs and 80ps pulse laser in selected materials: first in-situ and post-mortem analysis,” International Conference on Processing and Manufacturing of Advanced Materials, Paris 9-13 July 2018

[17] C. Phipps, “Performance test results for the laser-powered microthruster,” *AIP Conf. Proc.* **830**, 224-234 (2006)

[18] G. Tahan, S. Boyer, C. Phipps, L. Videau, M. Boustie, S. Oriol and C. Bonnal, “Laser propulsion: preliminary definition of a demonstrator,” paper 962, 8th European Conference for Aeronautics and Space Sciences, Madrid 1-4 July (2019)

[19] S. Bardy, B. Aubert, L. Berthe, P. Combis, D. Hébert, E. Lescoute, J.-L. Rullier and L. Videau, “Numerical study of laser ablation on aluminium for shock-wave applications: development of a suitable model by comparison with recent experiments,” *Opt. Eng.* **56**, 01104 (2016)

DOI: 10.13009/EUCASS2019-192

Appendix 1 : Symbol Glossary

Parameters

A_{eff}	Effective area of main optic $\pi D_{eff}^2/4$
A_s	Area viewed by receiver optic
a	Diffraction parameter ($4/\pi$ for Gaussian)
B	Background signal (W)
B_λ	Background spectral brightness (W/m^2/sterrad/μm)
B_{sig}	Background signal energy during t_g
c	Speed of light
C_m	Mechanical impulse coupling coefficient, N/W
d	Target diameter (m)
Ω_{rcv}	Receiver solid angle (sterrad) = A_{eff}/z^2
Ω_T	Target solid angle viewed from receiver (sterrad) = A_s/z^2
D	Actual transmit/receive main optic diameter (m)
D_{eff}	$0.9D_b$, effective diameter of main optic, reduced by apodization
d_p	Detector pixel diameter (m)
d_{pT}	Projected size of one detector pixel on target (m)
d_s	Laser beam spot size on target (m). By design, $d_s=d_{pT}$.
Φ	Laser fluence incident on target (J/m^2)
$\Delta\lambda$	Receiver bandwidth (μm)
$\Delta\lambda_L$	Laser bandwidth (μm)
η_e	Photoelectric efficiency = 85%
F	Main optic mirror focal length (m)
h	Planck constant
hc/λ	Photon energy (J)
I	Pulse intensity on target (W/m^2)
I_λ	Signal spectral brightness (W/m^2/sterrad/μm)
λ	Wavelength (m)
m	Number of encounters
M^2	Laser beam quality <=1
μ	Target mass areal density (kg/m^2)
N	Number of data samples per interaction
N_{pe}	Detector photoelectron number from target signal
R_λ	Target diffuse reflectance per sterradian
S	CW signal power (W)
S/B	Signal to background ratio
τ	Pulse duration (s)
τ_g	Detector gate duration (s)
w	Beam waist radius at focusing optic
w_o	Beam waist radius at focus
W	Laser pulse energy (J)
W_{sig}	Returned pulse energy (J)
z	Range (m)

DOI: 10.13009/EUCASS2019-192

Appendix 2 : Diffraction and Propagation

Diffraction and its effects the relationship between the laser beam waist at a focusing optic, w, and at focus, w_o, is accurately summarized, without approximations, by[1]

$$w_0 = \frac{w}{\left[1+\left(\frac{\pi w^2}{\lambda z}\right)^2\right]^{1/2}}. \tag{A1}$$

In terms of our parameters d_s & D_{eff} in the glossary this is equivalent to

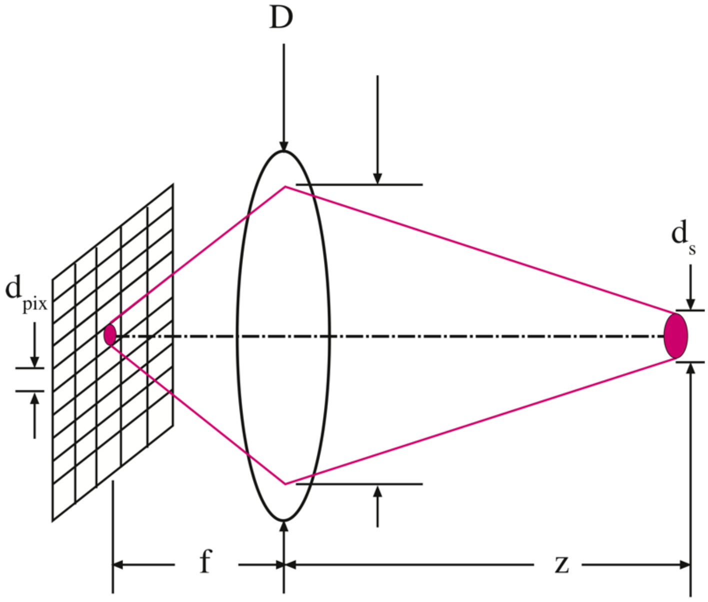

Figure 1. Illustrating focusing optic terms (not to scale)

$$d_s = \frac{D_{eff}}{\left[1+\left(\frac{A_{eff}}{M^2\lambda z}\right)^2\right]^{1/2}} \tag{A2}$$

for the spot diameter and effective optic diameter respectively. For spot area, we then have

$$A_s = \frac{A_{eff}}{\left[1+\left(\frac{A_{eff}}{M^2\lambda z}\right)^2\right]}. \tag{A3}$$

In normal situations, where $A_{eff} >> (M^2\lambda z)$, $A_s=(M^2\lambda z)^2/A_{eff}$ and we get the familiar relationship

$$d_s = \frac{4}{\pi}\frac{M^2\lambda z}{D_{eff}} \tag{A4}$$

for Gaussian beams. When z is of order several hundred km, Eq. (A3) is much more accurate.
For example, if z =1000km, M^2=2, A_{eff}=4m^2 and λ=1µm, Eq. (A3) gives A_s=0.8m^2, d_s=1.01m, but Eq. (A4) gives A_s=1.00m^2, a 20% error.

In Figure 1, for simplicity we have shown a lens for the focusing optic, but note that it is usually a mirror rather than a lens, and that the optic-to-detector array distance is very accurately equal to the focal length f when z is hundreds of km and f is of order 5m.

In this paper, we take d_{pT}=d_s also for simplicity.We can make this choice by design of the optic and the detector array.

Appendix 3. Passive Acquistion: Signal to Background & Photoelectron Count

In this section we use spectral brightness, which may be an unfamiliar term, but is critical when considering bandwidth limited systems such as the filtered detector we propose. Spectral brightness is intensity per unit sterradian and per micrometer span of the optical spectrum.

For the diffuse background in space from zodiacal light and diffuse galactic light, we use the values in Table A1.[2,3]

[1] F. L. Pedrotti and L. S. Pedrotti in *Introduction to Optics* (Prentice Hall, 1993) p. 461
[2] C. Phipps, "A laser-optical system to re-enter or lower low Earth orbit space debris," *Acta. Astron.* **93**, Table 14, p. 427 (2014)
[3] Ch. Leinert, et al., "The 1997 reference of diffuse night sky brightness," *Astron. Astrophys. Suppl. Ser.* **127**, 1-99 (1998)

DOI: 10.13009/EUCASS2019-192

Table A1: Assumed Spectral Brightness Values at 550nm

	Value	**Dimensions**
Diffuse Background in Space (Sun behind us, not looking at Earth or Moon B_λ	1.0E-6	W/(m^{2}sterrad μm)
Solar spectral brightness near Earth I_λ	1000	W/(m^{2}sterrad μm)
Target diffuse reflectivity into 1 sterrad R_λ	0.25	-----

For the background signal,

$$B=B_\lambda A_s\Delta\lambda\Omega_{rcv} = B_\lambda A_{eff}\Delta\lambda\ \Omega_T\ , \quad \textbf{(A5)}$$

the two products being equal by the étendue theorem. Similarly,

$$S = I_\lambda R_\lambda\ \Delta\lambda\Omega_T A_{eff} \quad \textbf{(A6)}$$

So $$\frac{S}{B}=\frac{I_\lambda R_\lambda}{B_\lambda}=2.5E8\ ,\ d_T>=d_s \quad \textbf{(A7)}$$

$$\frac{S}{B}=\frac{I_\lambda R_\lambda}{B_\lambda}\frac{d_T^2}{d_s^2}=2.5E8\frac{d_T^2}{d_s^2}\quad ,\ d_T<d_s.$$

In 6pE the example of Appendix 3, where z=1000km and d_s=0.45m, smaller targets will yield progressively worse S/B.
In staring mode, photoelectron current is

$$I_{pe}=\eta_e S/(hc/\lambda) \qquad \text{photoelectrons/s} \quad \textbf{(A8)}$$

For example, with a 45cm target at 1000km, a 50cm optic diameter and 1μm receiver bandwidth, S = 6pW and with η_e=85%, I_{pe}=1.47E7 photoelectrons/s. If, however, the target is moving across our field of view (before we can track it), an exposure time $\tau_{exp}= d_s/v_\perp$ is involved, during which it illuminates a single pixel. If $v_\perp$ =7.5km/s and d_s=1m, τ_{exp}= 130μs and N_{pe}=866 photoelectrons per pixel, a limiting factor.

$$N_{pe}=\tau_{exp}I_{pe} \quad \textbf{(A9)}$$

When there is a problem, the solution is to use shorter range for untracked targets, or to point where we know the target will be.

Appendix 4. Active Acquistion: Signal to Background & Photoelectron Count

With active acquisition,

$$I_\lambda=\frac{W}{A_s\tau\Delta\lambda_L} \qquad ,\ d_T>=d_s \quad \textbf{(A9)}$$

$$I_\lambda=\frac{W}{A_s\tau\Delta\lambda_L}(d_T^2/d_s{}^2) \qquad ,\ d_T<d_s, \quad \textbf{(A10)}$$

and Eq. (A7) still applies. For example, with a 1m target at 1000km, a 50cm optic diameter and 1μm receiver bandwidth with 550nm laser wavelength and η_e=85%, W=50mJ and τ=100ps, we have =20μW, B=1.2zW and S/B=8E14 during the pulse.

DOI: 10.13009/EUCASS2019-192

For signal energy, $$W_{sig} = I_\lambda R_\lambda \tau \Omega_T A_{eff} \Delta\lambda_L \quad \textbf{(A11)}$$

$$W_B = B\tau_g = B_\lambda \tau_g A_{eff} \Omega_T \Delta\lambda \quad \textbf{(A12)}$$

$$\frac{W_{sig}}{W_B} = \frac{I_\lambda \tau \Delta\lambda_L}{B_\lambda \tau_g \Delta\lambda} \quad \textbf{(A13)}$$

with the clear understanding that we may choose $\tau/\tau_g << 1$ and $\Delta\lambda_L << \Delta\lambda$. Using Eq. (A3) we have

$$\frac{S}{B} = \frac{I_\lambda R_\lambda}{B_\lambda}\frac{d_T^2}{d_s^2} = 2.5E8\frac{d_T^2}{d_s^2} \qquad d_T < d_s \quad \textbf{(A14)}$$

$$W_{sig} = W\frac{A_s}{z^2}\left[1 + \left(\frac{A_{eff}}{M^2 \lambda z}\right)^2\right](d_T / d_s)^2 \qquad d_T < d_s$$

For example, with λ=550nm, A_s = 0.16m^2, z = 1000km and other parameters as in the previous example, W_{sig}=2fJ. For photoelectrons we have

$$N_{pe} = W_{sig}\eta_e / (hc/\lambda) \quad \textbf{(A15)}$$

or 2.3E6 photoelectrons. Target transverse velocity is not relevant for such short pulses. In this case, d_s=45cm at 1000km.

If we take 4,680 photoelectrons as an acceptable signal (1.5% uncertainty) this means an acceptable signal is received for a 1cm target. However, we ignore this case because we have to track it first and we can't track such a small target with passive solar illumination.